

## CONTROL OF A DOUBLY FED INDUCTION GENERATOR AT GRID VOLTAGE IMBALANCE

TOMASZ ŁUSZCZYK, GRZEGORZ IWAŃSKI

Warsaw University of Technology, ul. Koszykowa 75, 00-662 Warszawa, Poland,  
e-mail addresses: tomasz.luszczuk@ee.pw.edu.pl, iwanskig@isep.pw.edu.pl

**Abstract:** Properties and control of a doubly fed induction machine operating under unbalanced grid voltage conditions have been presented. The proposed method does not include symmetrical sequences decomposition and is realized in a rotating frame not synchronized either with the grid voltage vector or with the stator flux vector. The method uses a reference torque and the reference  $q$  component of instantaneous power for calculation of the reference stator current. Next, calculation of magnetizing current for a given unbalanced grid voltage is used to assign the reference rotor current. Due to the fact that the reference current contains both a positive and a negative sequence, a proportional-integral-resonant controller is used. The main control target is the non-oscillatory waveform of torque, whereas other separate strategies like symmetrical stator current or sinusoidal rotor current can be easily obtained by adequate filtration of the reference control signals of the stator or rotor currents, respectively. The simulation results of the 2 MW model have been presented for a doubly fed induction generator as well as the results of laboratory tests with the use of a small scale 7.5 kW machine.

**Keywords:** *doubly fed induction generator, power and torque control, unbalanced grid*

### 1. INTRODUCTION

The doubly fed induction generator (DFIG) technology is mainly utilized in variable speed wind energy conversion systems [1, 2]. It is also known from large hydropower plants, internal combustion engine based generation units, and it is proposed in flywheel energy storage systems [3–5]. The main problem for this type of generators is their incapability of safe operation during severe voltage dips without a special protection circuit (crowbar) on the rotor side [6]. The rotor crowbar makes it possible to dump the machine's flux and reduces rotor induced voltage to the level acceptable for the rotor converter. However, during the operation of the crowbar, the power converter is disconnected. During the state of significant and permanent imbalance of grid voltage, the negative sequence voltage induced on the rotor side can be higher than that acceptable for the rotor power converter. This way, the generator should be permanently disconnected from the power grid until the grid voltage recovers to the normal condition [7].

However, for the low asymmetry factor of the grid voltage, operating points are possible in which the generator can work continuously and provide high quality energy.

From among possible separate targets related to machine control, three are most important: torque oscillations cancellation (strategy 1), symmetrical stator current (strategy 2), sinusoidal rotor current (strategy 3). Other strategies like constant  $pq$  components of instantaneous power producing an enormous amount of stator current harmonics, and a constant  $p$  component of power at sinusoidal stator current are possible [8]. However, in the course of these strategies, significant oscillations of electromagnetic torque occur, which can have a negative effect on mechanical components like gearboxes, bearings, etc. The paper focuses on the control method for the main strategy aimed at torque oscillations cancellation (strategy 1), which in an easy way can be modified to obtain the other two strategies. The analyzed structure of DFIG is shown in Fig. 1.

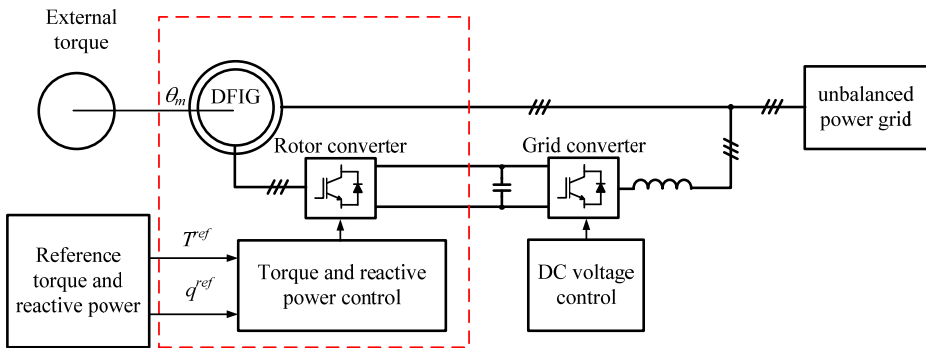


Fig. 1. General scheme of a doubly fed induction generator and a part of the system analyzed in the paper

The most popular control method for the doubly fed induction generator, realizing the mentioned control targets at unbalanced grid voltage operation, is vector control oriented to the stator flux (FOC). For the unbalanced grid operation mode, the classic FOC method has been modified by introducing separate control paths of positive and negative sequences with proportional-integral controllers [9–11]. The method requires decomposition of positive and negative sequences from measured stator and rotor currents, and stator (grid) voltage. Determination of symmetrical components requires precise calculation of the angle of a fundamental positive sequence grid voltage component. This solution is effective in the steady state, but it may provide slow responses during transients. Moreover, separation of the positive and negative sequence control paths of the stator or rotor current causes problems in rotor current limitation during voltage sags, because there are two pairs of orthogonal reference signals.

A similar solution with split control paths for positive and negative sequences of the rotor current is shown in [12]. The authors used positive sequence rotor current control with proportional-integral controllers, whereas the required  $pq$  power components oscillations or balanced stator current were realized by an additional parallel current con-

control path with so-called vector proportional-integral controllers VPI [13, 14]. Using this manner, two strategies can be reached by extraction of only the positive sequence of the stator current component without calculation of the negative sequence.

In [15], the reference current components for positive and negative sequences were transformed to common coordinates and added. This provides a common control path for both symmetrical components and a common regulator. Due to the occurrence of the negative sequence in the reference current, a 100 Hz oscillation occurs in reference signals in the  $dq$  frame due to the rotation of the coordinate system. Thus, parallel resonant terms were added to the proportional-integral controllers in each axis to improve the quality of the actual current. However, the calculation of the reference current still requires sequences decomposition.

The other method, well known in the literature, modified for the unbalanced grid operation of DFIG, is direct power control (DPC). A frontier publication in this field [16] presents DPC with hysteresis controllers of instantaneous  $pq$  power components with the decomposition of symmetrical components of the stator voltage. Constant and oscillatory power components required for specific control targets are controlled independently. Control of the oscillatory component is realized through the introduced factor  $k$ . Depending on this factor, it is possible to obtain non-oscillatory electromagnetic torque ( $k = -1$ ), symmetrical and sinusoidal stator current ( $k = 0$ ), constant stator power components ( $k = 1$ ), and intermediary states including sinusoidal rotor current.

Hu et al. [17] assumed constant angular speed of the stator flux vector, and constant shift between the stator flux vector and the stator voltage vector, which is true only for balanced grid voltage. It was assumed [18] that the derivative of the grid voltage  $\alpha$  component has the same phase as the  $\beta$  voltage component scaled by pulsation  $\omega_s$ , and analogously, the derivative of the  $\beta$  component equals the grid voltage  $\alpha$  component scaled by pulsation  $\omega_s$ , which is true only for some types of grid voltage asymmetries, but not for all, because grid voltage components  $\alpha$  and  $\beta$  may have different amplitudes or the phase shift between them may be different than  $\pi/2$  for some types of imbalance.

Zhou et al. [19] modified the basic structure of DPC for unbalanced grid operating conditions by adding resonant terms in  $pq$  power controllers. Thus  $pq$  power components oscillations can be eliminated, but the stator current is strongly nonlinear, and electromagnetic torque oscillations are enormous even for a relatively small asymmetry factor of the grid voltage. It is unacceptable in practice, most authors treat it as a background case which must be improved. The control method was further modified by Nian et al. [20] through calculation of reference  $pq$  power components correction signals using decomposition of grid voltage and stator current symmetrical sequences to obtain all described control targets. However, the used equations were still true only for the case of balanced grid voltage.

In the literature, several methods can be found which are equally effective due to implementation of resonant terms to keep the same shape of the actual stator or rotor current as reference signals. However, lack of sequence decomposition structures and

synchronization of the rotating frames simplifies the control method, and this is the main aim of the control system proposed in this paper. The method introduces calculation of reference signals of the stator current on the basis of reference reactive power and torque. Next, by calculation of magnetizing current at grid voltage imbalance, the reference rotor current signals are derived. Introducing low pass filters of  $dq$  frame oriented reference stator or rotor current, a symmetrical stator current strategy or symmetrical rotor current strategy are obtained.

The second chapter includes a description of the mathematical model. The third chapter presents derivation of stator and rotor current reference signals to obtain selected strategies of control. The fourth chapter presents simulation results of the 2 MW model of the doubly fed induction machine, whereas the fifth chapter presents experimental results with the 7.5 kW model.

## 2. MODEL OF DFIG WITH UNBALANCED STATOR VOLTAGE

### 2.1. MODEL EQUATIONS

The model of the doubly fed induction machine with variables referenced to the stator side is given by voltage and flux equations (1)–(4)

$$\overline{u}_s = R_s \overline{i}_s + \frac{d\overline{\psi}_s}{dt} + j\omega_s \overline{\psi}_s \quad (1)$$

$$\overline{u}_r = R_r \overline{i}_r + \frac{d\overline{\psi}_r}{dt} + j\omega_r \overline{\psi}_r \quad (2)$$

$$\overline{\psi}_s = L_s \overline{i}_s + L_m \overline{i}_r \quad (3)$$

$$\overline{\psi}_r = L_r \overline{i}_r + L_m \overline{i}_s \quad (4)$$

and stator flux can also be calculated by (5)

$$\overline{\psi}_s = \int (\overline{u}_s - R_s \overline{i}_s) dt + \overline{\psi}_s^0 \quad (5)$$

where  $\overline{u}_s, \overline{u}_r, \overline{i}_s, \overline{i}_r, \overline{\psi}_s, \overline{\psi}_r$  are the space vectors of stator and rotor voltage, current and flux respectively,  $R_s, R_r, L_s, L_r, L_m$  are respectively stator and rotor resistances, stator and rotor self inductances, and magnetizing inductance,  $\omega_s$  is the angular speed of the reference frame,  $\omega_r$  is the angular speed of the rotor related to the frame.

One of the possible torque equations used for elaboration of the control method with the use of variables represented in a rotating frame is given by (6), while the instantaneous power  $pq$  components are given by (7), (8). The equation (6) of electromagnetic

torque is chosen from among several possible, because the torque is described using stator current vector components. Using this equation (6) and  $q$  stator power equation (8), it is possible to find stator current components using reference signals of torque and  $q$  component of stator power.

$$T = \frac{3}{2} p_p \operatorname{Im} \left\{ \vec{\psi}_s \cdot \vec{i}_s^* \right\} = \frac{3}{2} p_p \left( \psi_{sd} i_{sq} - \psi_{sq} i_{sd} \right) \quad (6)$$

$$p_s = \frac{3}{2} \operatorname{Re} \left\{ \vec{u}_s \cdot \vec{i}_s^* \right\} = \frac{3}{2} \left( u_{sd} i_{sd} + u_{sq} i_{sq} \right) \quad (7)$$

$$q_s = \frac{3}{2} \operatorname{Im} \left\{ \vec{u}_s \cdot \vec{i}_s^* \right\} = \frac{3}{2} \left( u_{sq} i_{sd} - u_{sd} i_{sq} \right) \quad (8)$$

where  $T$  is the electromagnetic torque,  $p_s, q_s$  – components of instantaneous power by Akagi [21],  $p_p$  – number of poles pairs,  $u_{sd}, u_{sq}$  – grid voltage vector components,  $i_{sd}, i_{sq}$  – stator current vector components,  $\psi_{sd}, \psi_{sq}$  – stator flux vector components.

## 2.2. STATOR FLUX ESTIMATION

Estimation of the stator flux from (5) requires elimination of the constant component caused by offsets of voltage and current sensors, and elimination of the constant component caused by an unknown initial value of the flux. An equivalent solution is a first-order low pass filter with low cut-off frequency. However, such a filter, often used instead of integration in cage induction machine control, does not assure 90° phase shift between respective components of stator voltage and stator flux. Phase correctors can be used for the obtained stator flux components signals by additional rotation of the vector in the direction opposite to the natural rotation of the vector. However, under stator voltage imbalance, the phase shift between the positive sequence component of voltage and flux has the opposite sign than the phase shift between negative sequence components of these vectors. Thus, the phase corrections for the positive sequence and for the negative sequence are opposite. To introduce adequate phase correction for both symmetrical components of flux, they should be determined separately using sequences decomposition.

An alternative method of flux estimation giving close to 90° phase shift between voltage and flux is a second-order band-pass filter, or second-order low pass filter (Fig. 2). A second-order low pass filter with cut-off pulsation equal to  $\omega_s$ , damping factor 1 and gain  $2\omega_s^{-1}$  replaces the integrator for 50 Hz (the same gain and phase shift as the integrator for 50 Hz). It has to be noted that this manner (Fig. 2) is valid only for almost constant frequency of the grid voltage and makes it possible to estimate the fundamental frequency component of the flux. It cannot be used in cage induction machines fed from the converters by variable frequency stator voltage.

The applied method of flux estimation assures  $90^\circ$  phase shift between flux and voltage  $\alpha\beta$  components but it does not provide full information about the flux in dynamic states caused by voltage sags. In the literature, there are methods giving information about the transient component of flux. One of them is to use an observer in which the PI controller introduces a correction signal originated from the current-flux model to the main flux estimator based on the voltage model. However, taking into consideration the transient components of flux, it will significantly reduce transients oscillations of the controlled electromagnetic torque, but it will introduce a worse quality of the stator current. Thus, in this paper the transient component of flux is not taken into consideration to keep high quality of the stator current in transient states.

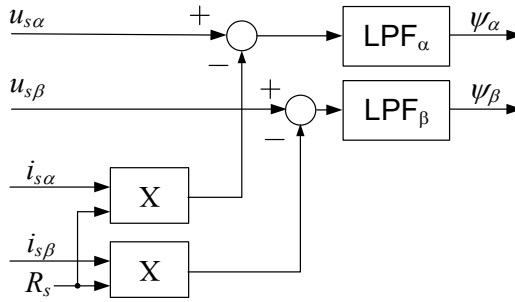


Fig. 2. Scheme of the stator flux components estimator with second-order low pass filter

Additionally, using only the fundamental frequency of the unbalanced stator flux (without harmonics), the method is less sensitive on the grid voltage harmonics, and the obtained stator current is more sinusoidal than the stator voltage in the case in which grid voltage contains higher harmonics. This will be shown in the experimental results section.

### 3. CONTROL METHOD FOR THE ROTOR CONVERTER

#### 3.1. ROTOR CURRENT REFERENCING FOR NON-OSCILLATORY TORQUE

Using the equations (6) and (8), the reference stator current vector components can be calculated based on reference torque  $T^{\text{ref}}$  and reference  $q_s^{\text{ref}}$  component of power.

$$i_{sd}^{\text{ref}} = \frac{2}{3} \frac{T^{\text{ref}} u_{sd} + q_s^{\text{ref}} p_p \psi_{sd}}{p_p (u_{sq} \psi_{sd} - u_{sd} \psi_{sq})} \quad (9)$$

$$i_{sq}^{\text{ref}} = \frac{2}{3} \frac{T^{\text{ref}} u_{sq} + q_s^{\text{ref}} p_p \psi_{sq}}{p_p (u_{sq} \psi_{sd} - u_{sd} \psi_{sq})} \quad (10)$$

The reference value of the controlled rotor current is given by the equation (11)

$$\overline{i_r^{\text{ref}}} = \overline{i_m} - \overline{i_s^{\text{ref}}} \quad (11)$$

Determination of the rotor reference current  $i_r^{\text{ref}}$  requires information about magnetizing current  $i_m$  of the machine at given grid voltage imbalance. The magnetizing current components can be reached by (12)(13).

$$i_{md} = \frac{\Psi_{sd} - L_{\sigma s} i_{sd}}{L_m} \quad (12)$$

$$i_{mq} = \frac{\Psi_{sq} - L_{\sigma s} i_{sq}}{L_m} \quad (13)$$

Replacing the stator current vector components  $i_{sd}$ ,  $i_{sq}$  in (12), (13) with reference signals  $i_{sd}^{\text{ref}}$ ,  $i_{sq}^{\text{ref}}$  to avoid measurement noises, and taking (11) into account, the reference value of rotor current vector components  $i_{rd}^{\text{ref}}$ ,  $i_{rq}^{\text{ref}}$  can be calculated by (14), (15).

$$i_{rd}^{\text{ref}} = \frac{\Psi_{sd} - L_{\sigma s} i_{sd}^{\text{ref}}}{L_m} - i_{sd}^{\text{ref}} = \frac{\Psi_{sd} - L_s i_{sd}^{\text{ref}}}{L_m} \quad (14)$$

$$i_{rq}^{\text{ref}} = \frac{\Psi_{sq} - L_{\sigma s} i_{sq}^{\text{ref}}}{L_m} - i_{sq}^{\text{ref}} = \frac{\Psi_{sq} - L_s i_{sq}^{\text{ref}}}{L_m} \quad (15)$$

### 3.2. ROTOR CURRENT CONTROL LOOP

For constant values of  $T^{\text{ref}}$  and  $q^{\text{ref}}$ , the stator current is sinusoidal, but unbalanced. In a  $dq$  rotating frame, the components of the reference current contain mainly the constant component and some amount of 100 Hz oscillating component representing a negative sequence. The usually applied proportional-integral term is too slow to eliminate a steady state error, so some improvements are made. In order to compensate for all disturbances caused by the negative sequence and couplings between the control paths, a full model of disturbances and decoupling terms is introduced [22]. It is obtained by inclusion of the stator voltage equation (1) and flux equations (3), (4) in the rotor voltage equation (2). Thus, the full model of the control plant, grid voltage disturbance and couplings between control paths is given by

$$\overline{u_r} = R_r \overline{i_r} + \sigma L_r \frac{d\overline{i_r}}{dt} + \frac{L_m}{L_s} \left( (\overline{u_s} - R_s \overline{i_s}) - j\omega_s (L_s \overline{i_s} + L_m \overline{i_r}) \right) + j\omega_r (L_r \overline{i_r} + L_m \overline{i_s}) \quad (16)$$

Decomposition of (16) to  $dq$  components and omission of terms representing a rotor current control plant provides rejection of disturbance and decoupling terms for each  $dq$  axis, respectively.

$$\begin{cases} \Delta u_{rd} = \frac{L_m}{L_s} \left( u_{sd} - R_s i_{sd} + \omega_s (L_s i_{sq} + L_m i_{rq}) \right) - \omega_r (L_r i_{rq} + L_m i_{sq}) \\ \Delta u_{rq} = \frac{L_m}{L_s} \left( u_{sq} - R_s i_{sq} - \omega_s (L_s i_{sd} + L_m i_{rd}) \right) + \omega_r (L_r i_{rd} + L_m i_{sd}) \end{cases} \quad (17)$$

Reference signals of the rotor current calculated on the basis of (14) and (15) contain 100 Hz oscillations. Due to relatively low gain of the PI controller at this frequency, the steady state error may not fully be eliminated. Thus, an additional term is introduced which can eliminate the 100 Hz component in the control error. To the PI controller, a resonant term is added, described by the transfer function in a continuous domain

$$G(s) = \frac{2K_r s}{s^2 + \omega_0^2} \quad (18)$$

Resonant terms used in the DFIG state controller require special attention during discretization and implementation in a digital signal controller. The shape of the resonant terms frequency characteristics, which has a very steep peak at resonant frequency, means that resonant terms should be discretized with great care. Yepes et al. [23] conducted an in-depth study of discretization methods of resonant terms, which is recommended to the reader for more information.

Discretization of continuous dynamic systems consists of finding such a discrete system which would respond to different stimuli as similar to its continuous equivalent as possible. The Tustin (bilinear) discretization is considered the best for resonant terms. However, using the basic version of this transformation results in the situation that frequency responses of the discretized and original systems are identical in shape but shifted along the frequency axis. It means that the resonant peak in the discrete resonant term is moved to another frequency. In order to compensate for this frequency shift, it is necessary to make a correction of the discretization method – called frequency pre-warping (19). The resonant pulsation  $\omega_0$  is set to 100 Hz

$$s = \frac{\omega_0}{\tan\left(\frac{\omega_0 T}{2}\right)} \frac{z-1}{z+1} \quad (19)$$

### 3.3. CONTROL SCHEME FOR THREE TARGETS

The way of rotor current reference calculation at non-oscillatory torque with simultaneous sinusoidal shape of the stator current (strategy 1) described in Subsection 3.1

can be modified in an easy way to obtain the two other targets mentioned in the introduction. The symmetrical stator current target (strategy 2) can be obtained by filtration of the oscillatory component from the reference stator current signals provided by (9) and (10). The sinusoidal rotor current target (strategy 3) can be reached by filtration of oscillatory components from the reference rotor current signals provided by (14) and (15). The strategies 1, 2, or 3 cannot be reached simultaneously, thus the introduced low pass filters are optional. Selection of the strategy can be made arbitrarily depending on the application. For wind turbines with gearboxes, the most wanted strategy is elimination of electromagnetic torque oscillations which are significant even for a relatively small amount of negative sequence components in the grid voltage. For big machines, the participation of magnetizing current in total stator or rotor current is insignificant, therefore strategies 2 and 3 related to symmetrical stator current and sinusoidal rotor current, respectively, give similar properties. Selection of the strategy can also be automated depending on the reach of maximum current in any phase of the stator in strategy 1. In this strategy, the stator current is unbalanced. Increase of the stator power causes that the stator current is also increased until one of the phase currents reaches the maximum. Then the strategy can be switched to another one (2 or 3) to make a further increase of the generated power possible. A scheme of the control method with low pass filters giving possible strategy 2 and 3 is shown in Fig. 3.

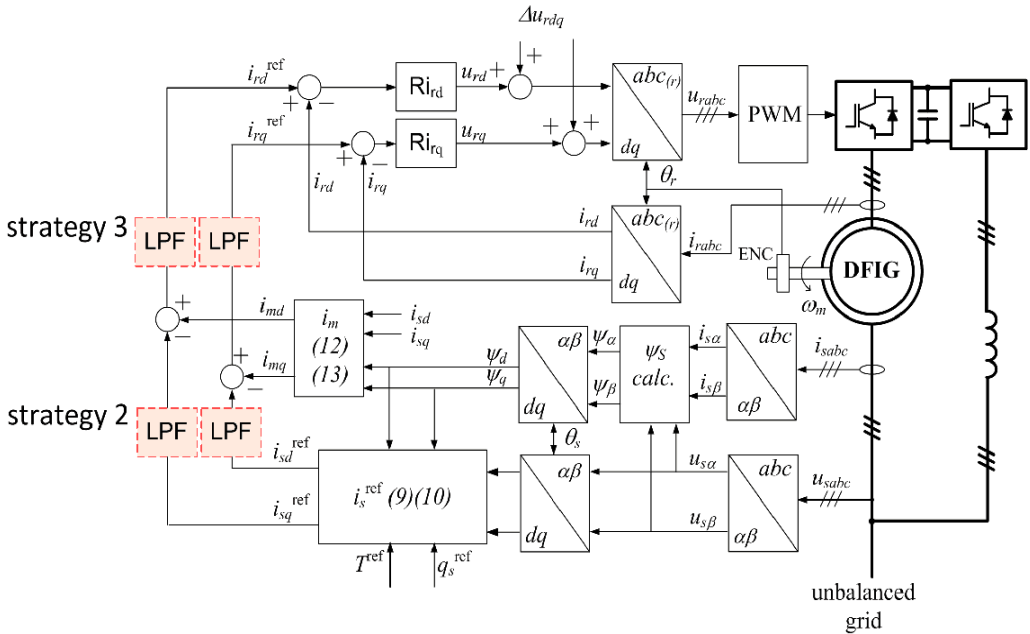


Fig. 3. Scheme of the control system for non-oscillatory torque (strategy 1) with optional low pass filters giving symmetrical stator current (strategy 2) or sinusoidal rotor current (strategy 3)

#### 4. SIMULATION RESULTS WITH THE 2 MW MACHINE MODEL

The proposed control method was verified in simulation tests with a model of a 2 MW doubly fed induction machine fed from continuous voltage sources and measured signals sampled with 2 k Hz. Simulation results in the steady state for rated torque are shown in Fig. 4. Figure 4a presents strategy 1 with a non-oscillatory torque and sinusoidal (but unbalanced) stator current, Fig. 4b shows strategy 2 with a symmetrical stator current, and Fig. 4c presents strategy 3 with a sinusoidal rotor current. All the assumed strategies are achieved. For large machines the amount of magnetizing current in the total rotor or stator current is low, so the difference between strategy 2 and strategy 3 is not significant.

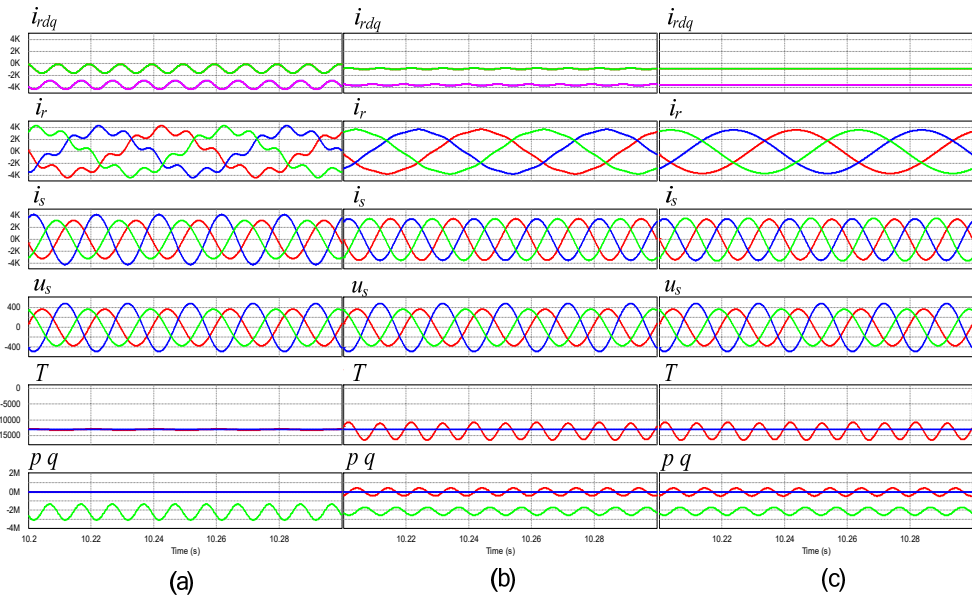


Fig. 4. Simulation results of the steady state for the rotor current control realizing: a) strategy 1 (non-oscillatory torque), b) strategy 2 (symmetrical stator current), c) strategy 3 (sinusoidal rotor current)

Simulation results for various electromagnetic torque  $T$  and  $q_s$  component of the instantaneous power at strategy 1 (non-oscillatory torque) are presented in Fig. 5. Simultaneously, the grid voltage frequency is set to 49.5 Hz to show that the proposed control is working correctly even if the resonant term set to 100 Hz is not matched precisely to the oscillations frequency, which in this case equals 99 Hz. For a 1 Hz deviation from the resonant frequency in a  $dq$  frame, gain of the resonant term is still high enough to significantly reduce the steady state error. Synchronization of the reference  $dq$  frame with the stator voltage or stator flux vector is not necessary, because the rotor current

vector components are calculated based on the reference torque and  $q$  component of the instantaneous power, which are independent of the coordinate frame.

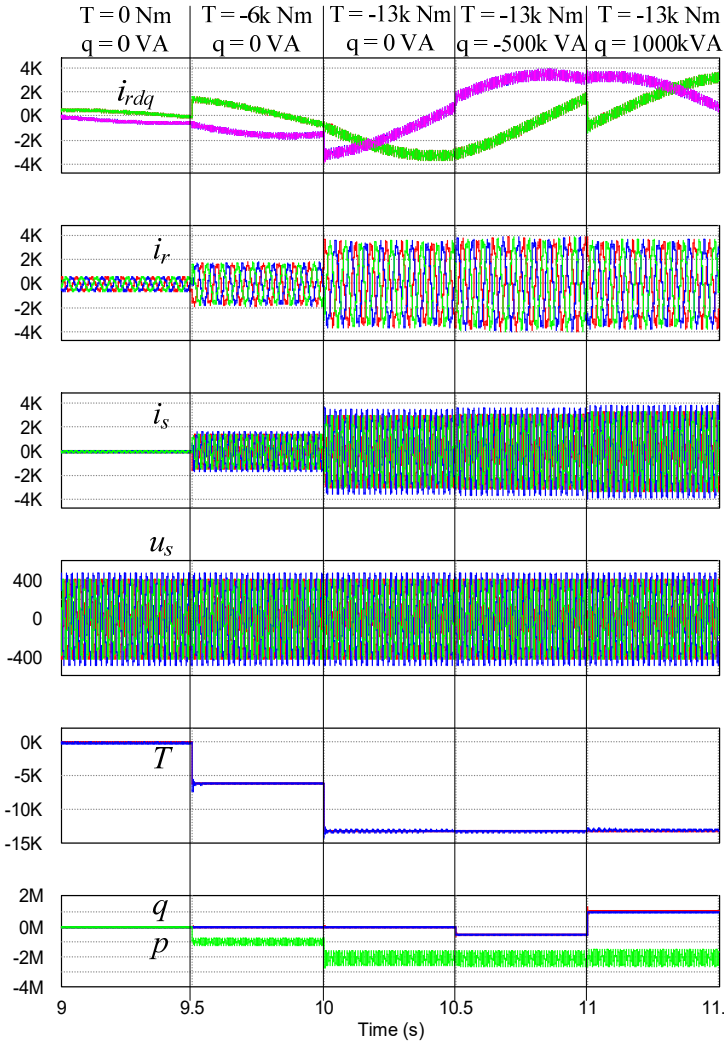


Fig. 5. Simulation results of the control method with the 2 MW model of a doubly fed induction machine realizing strategy 1 (non-oscillatory torque) at the grid voltage frequency equal to 49.5 Hz

The simulation with a high power machine is made, because this type of generator is used mainly in wind turbines in the power range from 1.5 MW to 3.3 MW. The simulation model uses continuous sources instead of a discrete model of a power electronic converter to make the simulation faster. The controller design (tuning) is made with the trial and error method. Analytical methods can be used for tuning but it does make sense

for more advanced simulation model with a switched power converter, with consideration of all nonlinearities like sampling of measured variables and delays between measurement and control action, as well as some noises and offsets of current and voltage transducers. The machine parameters are given in Table 1.

Table 1. Parameters of the 2 MW doubly fed induction machine model used in the simulation

Parameter	Value
Rated power, $P_n$	2 MW
Stator voltage, $U_{sn}$	690 V
Stator rated current, $I_{sn}$	1760 A
Stator/rotor turns ratio, $u$	0.34
Stator resistance, $R_s$	2.6 m $\Omega$
Rotor resistance, $R_r$	2.6 m $\Omega$
Stator leakage inductance, $L_{s\sigma}$	0.087 mH
Rotor leakage inductance, $L_{r\sigma}$	0.087 mH
Magnetizing inductance, $L_m$	2.5 mH
Number of poles pairs, $p_p$	2

## 5. EXPERIMENTAL RESULTS WITH A SMALL POWER MACHINE

Experiments were conducted in a laboratory unit with a small power of 7.5 kW machine. Parameters of the machine are given in Table 2.

Table 2. Parameters of the 7.5kW doubly fed induction machine model used in the laboratory tests

Parameter	Value
Rated power, $P_n$	7.5 MW
Stator voltage ( $\Delta/Y$ ), $U_{sn}$	220/380 V
Stator rated current ( $\Delta/Y$ ), $I_{sn}$	27.4/15.7 A
Stator/rotor turns ratio, $u$	2.088
Stator resistance, $R_s$	0.43 $\Omega$
Rotor resistance, $R_r$	0.71 $\Omega$
Stator leakage inductance, $L_{s\sigma}$	10 mH
Rotor leakage inductance, $L_{r\sigma}$	10 mH
Magnetizing inductance, $L_m$	120 mH
Number of poles pairs, $p_p$	2

The waveforms were recorded with a Yokogawa DL850 scope recorder. A control algorithm was implemented with a TMS320F28335 digital signal microprocessor. Figure 6 presents the scheme of the laboratory setup. The grid side converter equipped with a pre-charging circuit is responsible for DC link voltage control and it is controlled independently of the rotor side converter with the classic voltage oriented control method. It does not influence the stator and rotor current, as well as electromagnetic torque oscillations, therefore the description of the grid side converter control is omitted in the paper. Matching the transformer between the grid side converter and grid is to reduce the voltage of the DC link, as according to the DFIG parameters from Table 2, the rotor voltage is significantly smaller than stator voltage. The grid transformer is a multi-tap device that allows one to create stator voltage imbalances.

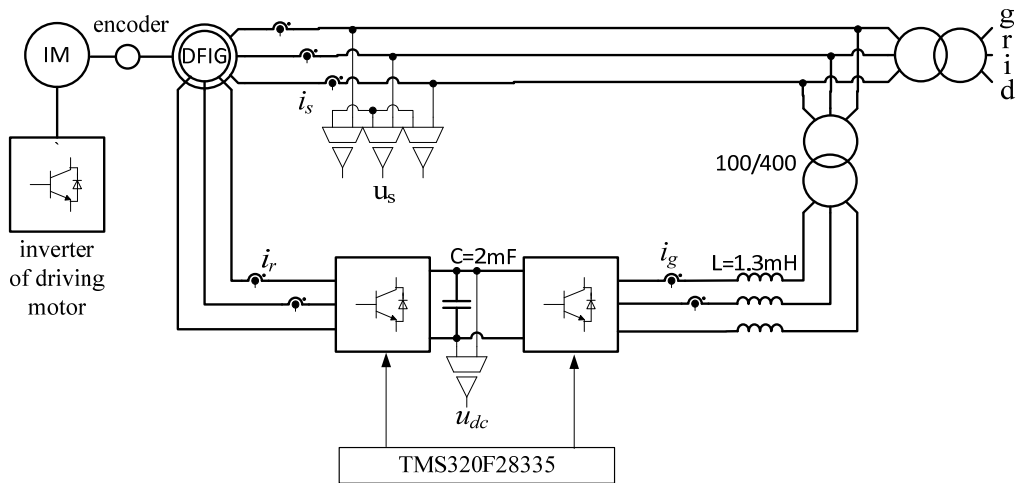


Fig. 6. Scheme of the laboratory setup with the doubly fed induction generator

The switching and sampling frequency in the laboratory tests equals 4 kHz, and the speed range set for driving the induction machine is from 1200 to 1800 rpm ( $\pm 20\%$  around the synchronous speed).

Figure 7 presents oscillograms recorded during steady states of non-oscillatory torque strategy (Fig. 7a), symmetrical stator current strategy (Fig. 7b), and sinusoidal rotor current strategy (Fig. 7c). A hodograph of the voltage vector is not perfectly elliptic due to harmonics distortions, although current vectors hodographs are elliptic or circular. It means that grid voltage harmonics have little influence on the current quality when the proposed method is used.

Figure 8 presents oscillograms and current vectors hodographs during zeroed stator current (Fig. 8a) or zeroed rotor current (Fig. 8b), respectively. It shows that the control method operates in a stable way in different modes.

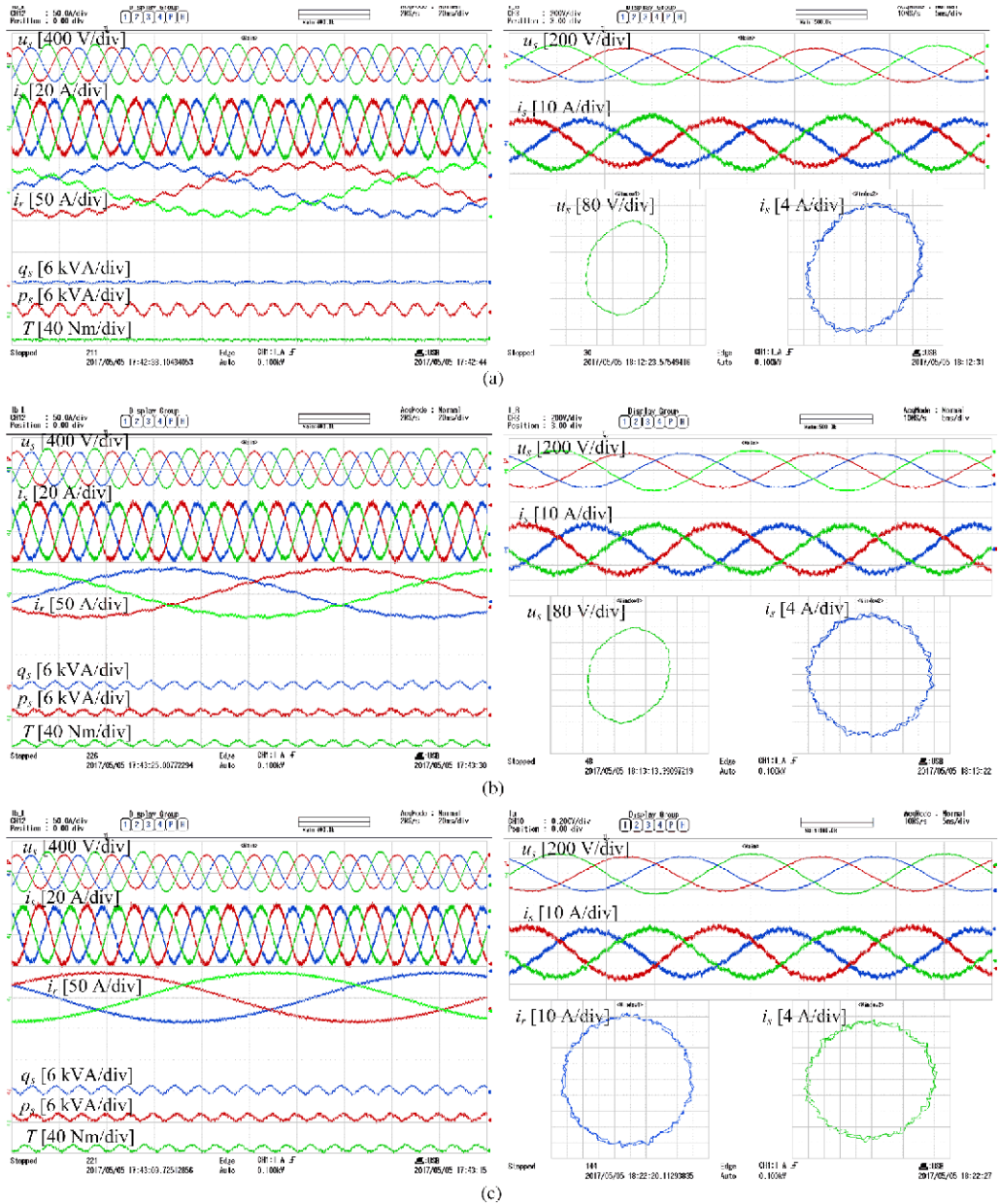


Fig. 7. Oscilloscopes presenting steady states obtained from the laboratory unit at: a) non-oscillatory torque strategy, b) symmetrical stator current strategy, c) sinusoidal rotor current strategy

Figure 9 presents oscilloscopes with a fast response to step change of reference torque. Such fast response is possible thanks to the adequate disturbance rejection model

and decoupling terms. Small oscillations on the  $q$  component of power in Fig. 7a and Fig. 9 occur due to the assumed linearity of the magnetic circuit and imprecise calculation of the real magnetizing current.

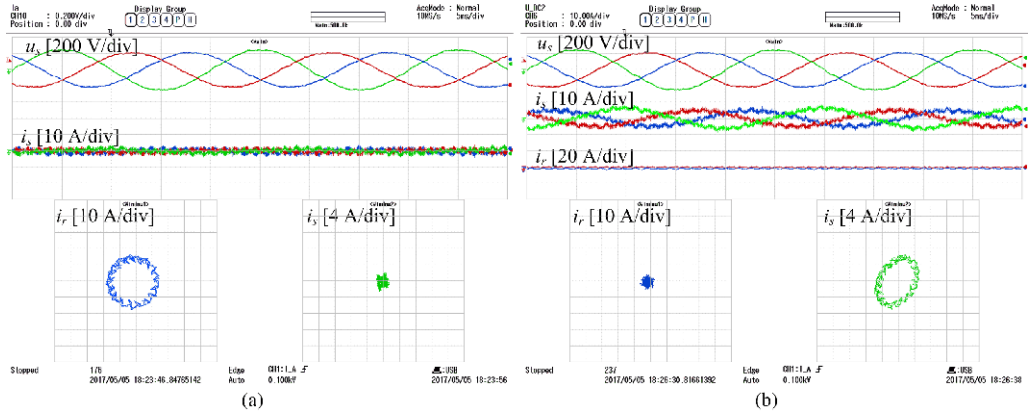


Fig. 8. Oscilloscopes presenting operation of a doubly fed induction machine at: a) zeroed stator current, and b) zeroed rotor current

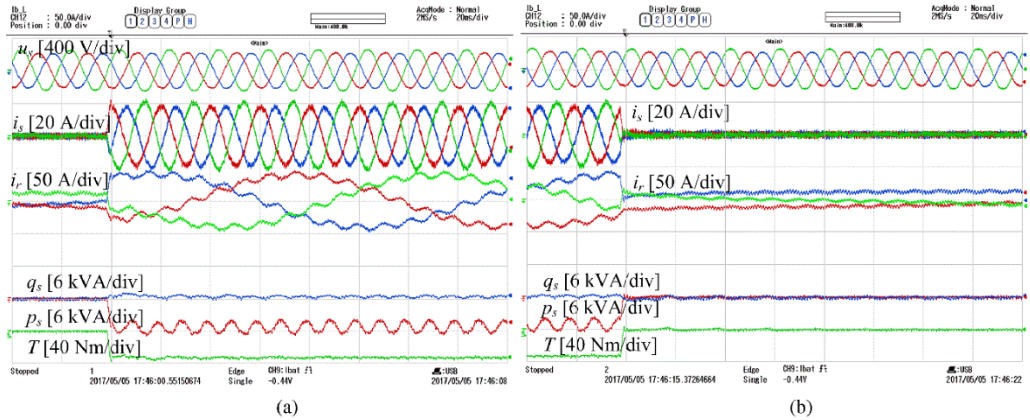


Fig. 9. Oscilloscopes presenting transient states of non-oscillatory torque strategy at: a) step loading, and b) step unloading

Figure 10 presents operation of the doubly fed induction machine at a grid voltage imbalance and variable rotor speed for non-oscillatory reference torque. It can be seen that waveforms of torque, and stator power  $p$  $q$  components do not depend on the rotor speed. Figure 11 presents the response of the machine to 10% asymmetrical grid voltage sag. Initially, after a change of grid voltage, there are short transient oscillations on the torque  $T$  and  $q$  component of power signals. This is caused by omission of the transient

component in the calculated flux. However, thanks to this manner, the stator current keeps its sinusoidal shape during transients.

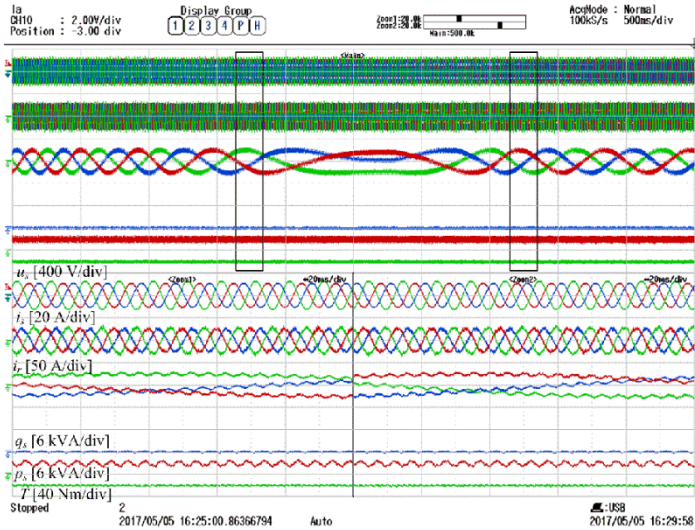


Fig. 10. Oscillograms presenting transient states of non-oscillatory torque strategy at a variable rotor speed

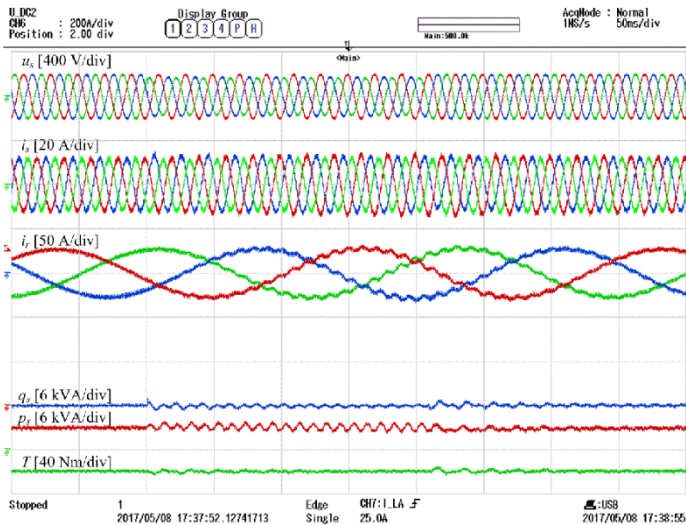


Fig. 11. Oscillograms presenting transient states of non-oscillatory torque strategy at a grid voltage asymmetrical sag with a 10% asymmetry factor

## 6. CONCLUSION

The proposed method of torque and  $q$  component of instantaneous power control works without the phase locked loop and decomposition of symmetrical components. It keeps constant controlled variables with small short oscillations during transients. A fast response to step change of reference torque can be reached through the full model of disturbance rejection and decoupling terms. Three different targets such as non-oscillatory torque, symmetrical stator current or sinusoidal rotor current can be obtained by simple filtration of the reference current signals. Due to high gain of the current controller around resonant frequency, current controllers compensate for steady state error even during small deviations of grid voltage frequency.

Future work can focus on the doubly fed induction generator operation with distorted grid. The presented equations for stator and rotor current reference calculation are general and do not assume sinusoidal waveform of the stator voltage. However, the proposed way of flux calculation gives accurate results only for 50 Hz and to obtain a real waveform of the flux, another method of flux estimation must be proposed to fully eliminate electromagnetic torque oscillations. A separate issue is related to the reference  $q$  component. The same electromagnetic torque can be achieved for a different waveform of the  $q$  component of power, so for a different waveforms of stator and rotor currents.

## ACKNOWLEDGMENTS

The work is supported by the statutory funds of the Faculty of Electrical Engineering of the Warsaw University of Technology.

## REFERENCES

- [1] LISERRE M., CARDENAS R., MOLINAS M., RODRIGUEZ J., *Overview of multi-MW wind turbines and wind parks*, IEEE Trans. Ind. Electron., 2011, 58(4), 1081–1095.
- [2] MÜLLER S., DEICKE M., DE DONCKER R., *Doubly fed induction generator systems for wind turbines*, Ind. Appl. Mag. IEEE, 2002, 8(3), 26–33.
- [3] KUWABARA T., SHIBUYA A., FURUTA H., KITA E., MITSUHASHI K., *Design and dynamic response characteristics of 400 MW adjustable speed pumped storage unit for Ohkawachi Power Station*, IEEE Trans. Energy Convers., 1996, 11(2), 376–382.
- [4] WARIS T., NAYAR C.V., *Variable speed constant frequency diesel power conversion system using doubly fed induction generator (DFIG)*, 2008 IEEE Power Electronics Specialists Conference, 2008, 2728–2734.
- [5] AKAGI H., SATO H., *Control and performance of a doubly-fed induction machine intended for a flywheel energy storage system* IEEE Trans. Power Electron., 2002, 17(1), 109–116.
- [6] PANNELL G., ATKINSON D.J., ZAHAWI B., *Minimum-threshold crowbar for a fault-ride-through grid-code-compliant dfig wind turbine*, IEEE Trans. En. Conv., 2010, 25(3), 750–759.
- [7] GENG H., LIU C., YANG G., *LVRT capability of DFIG-based WECS under asymmetrical grid fault condition*, IEEE Trans. Ind. Electron., 2013, 60(6), 2495–2509.

- [8] SANTOS-MARTIN D., RODRIGUEZ-AMENEDO J.L., ARNALTE S., *Direct power control applied to doubly fed induction generator under unbalanced grid voltage conditions*, IEEE Trans. Power Electron., 2008, 23(5), 2328–2336.
- [9] KIM Y., LEE D., *Active and reactive power control of DFIG for wind energy conversion under unbalanced grid voltage*, 5th Int. Power Electron. Motion Control Conf. IPEMC '06, 2006.
- [10] QIAO W., HARLEY R.G., *Improved control of DFIG wind turbines for operation with unbalanced network voltages*, Conf. Rec. IAS Ann. Meet. IEEE Ind. Appl. Soc., 2008, 1–7.
- [11] XU L., WANG Y., *Dynamic modeling and control of DFIG-based wind turbines under unbalanced network conditions*, IEEE Trans. Power Syst., 2007, 22(1), 314–323.
- [12] SONG Y., NIAN H., *Modularized control strategy and performance analysis of DFIG system under unbalanced and harmonic grid voltage*, IEEE Trans. Power Electron., 2015, 30(9), 4831–4842.
- [13] LASCU C., ASIMINOAEI L., BOLDEA I., BLAABJERG F., *High performance current controller for selective harmonic compensation in active power filters*, IEEE Trans. Power Electron., 2007, 22(5), 1826–1835.
- [14] SONG Y., ZHOU D., BLAABJERG F., *Impedance based analysis of DFIG stator current unbalance and distortion suppression strategies*, Industrial Electron. Conf., 2016, 4151–4157.
- [15] HU J., HE Y., XU L., WILLIAMS B.W., *Improved control of DFIG systems during network unbalance using PI-R current regulators*, IEEE Trans. Ind. Electron., 2009, 56(2), 439–451.
- [16] SANTOS-MARTIN D., RODRIGUEZ-AMENEDO J.L., ARNALTE S., *Direct power control applied to doubly fed induction generator under unbalanced grid voltage conditions*, IEEE Trans. Power Electron., 2008, 23(5), 2328–2336.
- [17] HU J., ZHU J., DORRELL D.G., *Predictive direct power control of doubly fed induction generators under unbalanced grid voltage conditions for power quality improvement*, IEEE Trans. Sustain. Energy, 2015, 6(3), 943–950.
- [18] SHANG L., HU J., *Sliding-mode-based direct power control of grid-connected wind-turbine-driven doubly fed induction generators under unbalanced grid voltage conditions*, IEEE Trans. En. Conv., 2012, 27(2), 362–373.
- [19] ZHOU P., HE Y., SU D., *Improved direct power control of a DFIG-based wind turbine during network unbalance*, IEEE Trans. Power Electron., 2009, 24(11), 2465–2474.
- [20] NIAN H., SONG Y., ZHOU P., HE Y., *Improved direct power control of a wind turbine driven doubly fed induction generator during transient grid voltage unbalance*, IEEE Trans. En. Conv., 2011, 26(3), 976–986.
- [21] AKAGI H., KANAZAWA Y., NABAE A., *Generalized theory of the instantaneous reactive power in three-phase circuits*, Int. Power Electronics Conf., 1983, 1375–1386.
- [22] ŁUSZCZYK T., IWAŃSKI G., *Comparison of decoupling structures in a rotor current control of doubly fed induction generator*, 8th Int. Conf. Exhib. on Ecological Vehicles and Renewable Energies EVER '13, 2013, Monte Carlo, Monaco, 1–5.
- [23] YEPES A.G., FREIJEDO F.D., LOPEZ Ó., DOVAL-GANDOY J., *High-performance digital resonant controllers implemented with two integrators*, IEEE Trans. Power Electron., 2011, 26(2), 563–576.